Capacity and Error Performance Verification of Multi-Antenna Schemes in Radio-over-Fiber Distributed Antenna System

Anthony E. Aighobahi, *Student Member, IEEE*, and Nathan J. Gomes, *Senior Member, IEEE*

Abstract **A radio-over-fiber distributed antenna system permits larger physical separation between antennas in a wireless system's infrastructure; this investigation verifies that improved performance – lower error rates and higher capacities – can thus be achieved. In this paper, specific single-input multiple-output (SIMO), multiple-input single-output (MISO) and multiple-input multiple-output (MIMO) algorithms are *compared* in an experimental radio over fiber system, using user-defined processing functions for the signals. It is shown that significantly reduced symbol error rate (SER) and modestly increased capacity is achieved for a wireless 1x2 SIMO uplink using the maximal ratio combining (MRC) processing algorithm and 2x1 MISO downlink using the Alamouti space time block coding (STBC) scheme. Further, SER is reduced for a downlink 2x2 wireless MIMO using the zero-forcing algorithm while, most importantly, greatly increased capacity is achieved through the spatial multiplexing gain.**

***Index Terms*—Distributed antenna system (DAS), Radio-over-Fiber (RoF) system, multiple-input multiple-output (MIMO), maximum-ratio combing, space-time block coding, zero-forcing**

I. Introduction

The increasing demand for higher data rate by growing numbers of mobile users [1] has made it necessary to develop systems that will improve wireless coverage and capacity. 80%-90% of mobile data traffic originates from the indoor environment [2], and more traffic will be offloaded from cellular networks on to indoor wireless networks increasing their need to offer high data rates. Approaches to enable this include femtocells, relays and distributed antenna systems (DAS).

In DAS, remote antenna units (RAUs) are geographically deployed and connected to a central unit (CU) using either an out band radio link, coaxial cables, a digital optical network or radio-over-fiber (RoF) links to extend the indoor wireless coverage from the base station and to share the hardware and bandwidth resources [3]. DAS has attracted much attention [4-6] for the in-building environment because it can provide high quality signal coverage, with low interference and high signal-to-noise ratio (SNR). Also, DAS can facilitate easy upgrade of existing services to emerging wireless services due to its centralized architecture [7] making it easier to adopt

Manuscript received January 15, 2016; revised May 03, 2016

The authors are with Communications Research Group, School of Engineering and Digital Arts, University of Kent, Canterbury, Kent CT2 7NT, UK (e-mail: aea25@kent.ac.uk and n.j.gomes@kent.ac.uk).

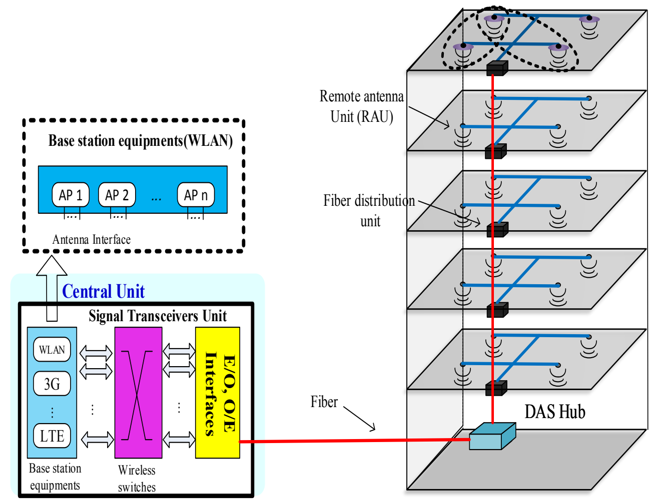

Fig.1 RoF-based Distributed Antenna System (DAS) [8]

different techniques such as higher order modulation, orthogonal frequency-division multiplexing (OFDM), advanced coding schemes and, more recently, multiple-input multiple-output (MIMO) schemes to widely improve wireless access rates.

Fig. 1 shows an illustrative RoF-based DAS infrastructure used to distribute wireless local area network (WLAN) signals and mobile telephone signals (3G, Long Term Evolution (LTE). In a RoF system setup, the analog signal is modulated onto a laser diode and transmitted via optical fiber to a photodiode receiver thereafter; the signal is amplified for wireless transmission. Using RoF links in DAS has key advantages, such as simple configuration and low loss of optical fiber to improve signal transmission, and when using simple direct modulated laser and direct detection photodiode (PD), the infrastructure cost can be reduced [9]. The RAUs are merely a distributed set of antennas, with little or no processing capability, that exchange radio frequency (RF) signals with the CU where all the signal processing such as modulation, demodulation, multiplexing, de-multiplexing, handover, diversity and protocol transformations are carried out [10].

II. Multi-Antenna Schemes for RoF-DAS

Multi-antenna schemes exploit multipath propagation and improve performance, for example reducing the fading problem experienced by conventional wireless systems where the received signal level varies. They have been adopted in most new wireless communication standards, such as WiFi, LTE and WiMAX, to provide increased capacity and ensure reliability and speed. The integration of RoF-DAS and multi-antenna schemes can further bring about improvement in throughput performance taking advantage of the largely separated multiple RAUs.

Previous work on RoF-DAS for improving MIMO systems was presented in [11]; high throughput was maintained in an experimental RoF-DAS-supported MIMO system, especially with widely separated antennas. In [12], it was shown that while an RoF-supported 3x3 MIMO system increased throughput from 201 Mbps to 475 Mbps compared to a SISO system when the antennas were closely separated, further improvement to 530 Mbps was achieved when the antenna elements were separated by 4-m. Also, an investigation was carried out in [8] to determine the throughput of a commercial MIMO access point in DAS with different fiber lengths, the results indicating that high throughput can be maintained even when the fiber length difference between the RAUs is 100m. However, these works were based on commercial products and the specific MIMO algorithms used within these products were unknown. Other papers have used specific multi-antenna algorithms in RoF-DAS. For example, a precoding algorithm was demonstrated in [13] to show that centralized joint/cooperative processing can provide significant gains when compared to non-cooperative transmission. In [14], a space-frequency block coding (SFBC) scheme was used in MISO to show improved performance over single antenna transmission.

In [15], we experimentally investigated the benefits of the Maximal Ratio Combining (MRC*)* algorithm in the RoF-DAS uplink with one transmitting mobile unit placed at different locations in a typical office environment and the OFDM signals gathered through two RAUs and brought back to the central unit for processing (a 1x2 SIMO scheme). It was shown that using the fiber-connected DAS infrastructure enabled an EVM reduction from around 10% to around 8%, when the distance between RAUs was 0.3-m, with further reductions to 6% and 4%, when inter-RAU distances were 2-m and 4-m, respectively, compared to a single RAU.

Here, we extend the work to investigate the symbol error rate (SER) for the MRC algorithm. In addition, we investigate the potential benefit of the space time block coding (STBC) Alamouti algorithm in the RoF-DAS downlink where signals from two transmitting RAUs are encoded and sent to one receiving mobile unit (2x1 MISO scheme). It should be noted that the Alamouti algorithm was developed to achieve the same spatial diversity order as MRC, but with complexity moved from receiver to transmitter, and relies on the signals transmitted by the antenna elements being sufficiently uncorrelated: this should be enabled by the RoF DAS. Then, the effect of the greater channel decorrelation with two separated RAUs in a RoF-DAS each transmitting independent streams of data to one mobile unit with two receiving antennas (2 x 2 MIMO) using the zero-forcing (ZF) algorithm to remove intersymbol interference (ISI) is investigated.

In this paper, we *compare* MRC SIMO, STBC MISO and ZF MIMO algorithms in RoF-DAS. The theory of the metrics used to characterize the performance of the system and the selected multi-antenna algorithms used are described in Section III while Section IV explains the experimental setup, and in Section V measurements results are discussed. The conclusion follows, in Section VI.

III. Theory

A. Error probability

The error introduced into the system by the RoF link or wireless channel is often evaluated in terms of error vector magnitude (EVM), effectively a measure of signal-to-noise ratio (SNR). EVM is typically expressed in decibels (dB) or a corresponding percentage and a minimum limit is often specified in advanced radio systems with complex modulation schemes. The EVM limits for wireless local area network (WLAN) modulation scheme for 16-QAM is 11.2%, 64-QAM is 6.5% and 256-QAM is 3.1% [16]

Unlike EVM, the error rate determines the error count in the data received. The error rate can be counted in terms of bits (BER) or symbols (SER). BER or SER is measured after the QAM demodulation.

B. Channel Capacity

The capacity determines the data rate that can be transmitted through the channel with small probability of error. It can be calculated based on the measured complex channel transfer matrix $\boldsymbol{H}$ obtained from channel state information (CSI) estimated at the receiver for every n transmit and m receive antenna pair. When the complex channel transfer matrix $\boldsymbol{H}$ is measured, its singular value decomposition (SDV) values are used to calculate the channel capacity of the MIMO ($C_{\mathbf{MIMO}}$**)** scheme. This is given by an extended Shannon capacity equation as [17]:

$$C_{MIMO} = \log_2 \det \left(I_{NR} + \frac{\boldsymbol{\rho}}{\boldsymbol{N_T}} \, \mathbf{H}\mathbf{H}^{\mathbf{H}} \right) \ \text{bps/Hz} \qquad (1)$$

where $\mathbf{N}_{T}$ is the number of transmit antennas and $\boldsymbol{\rho}$ is the SNR. In this paper we used the measured modulated error rate (MER) as SNR. MER and SNR can be used interchangeably [18] since MER is the ratio of average signal constellation power to average constellation error power, therefore, MER is digital complex baseband signal-to-noise-ratio (SNR).
The MIMO capacity in equation (1) reduces to the following expression for SIMO capacity (C_{SIMO}) [19]:

$$C_{SIMO} = \log_2 (1 + \mathbf{N_R}\, \rho) \quad \text{bps/Hz} \qquad (2)$$

Here, MER ρ is multiplied by a factor of $\mathbf{N_R}$ representing the total received power accumulated in the single degree of freedom of the channel

The capacity of a MISO channel (C_{MISO}) which is the same as SISO is [19]:

$$C_{MISO} = \log_2 (1 + \rho) \quad \text{bps/Hz} \qquad (3)$$

C. Selected multi-antenna algorithms

Multi-antenna schemes enhance performance compared to single-input single-output (SISO) systems; they can be broadly classified into spatial diversity techniques (used to improve data reliability in SIMO and MISO schemes) and spatial multiplexing techniques (used to increase data rates) [20]. These techniques use different coded algorithms. For SIMO, the received signals in the different antennas can be combined

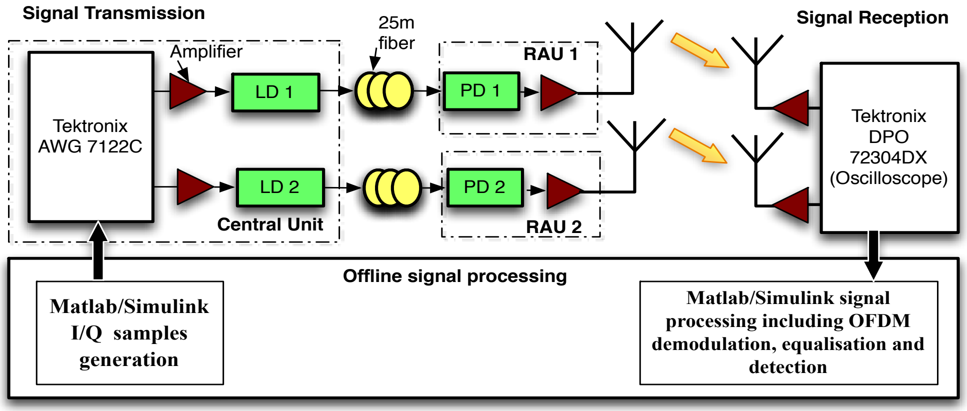

Fig. 2 The downlink Experimental setup for 2x2 MIMO over Fiber. PD=Photodetector, LD=laser diode, RAU=Remote antenna unit

using selection combining (SC), maximal ratio combining (MRC) or equal gain combining (EGC).

MRC achieves the best performance in the sense that it maximizes the post-combining SNR. In our SIMO experiment, we modified the MRC script in program 10.1 of [20] using MATLAB/Simulink software to combine the baseband signals received by two RAUs. Each received signal branch is multiplied by a weight factor, which is the signal amplitude thereby amplifying the better signal and attenuating the poorer signal. This algorithm has been experimentally demonstrated in [21, 22] to show improved performance to the SISO system but not in a DAS or RoF-supported system.

Space-time block coding (STBC) algorithms are used in downlink MISO schemes to encode signals transmitted by multiple antennas. Alamouti coding [23] is the most attractive STBC algorithm because it is simple and does not require feedback of channel state information to the transmitter. The encoded signals using Alamouti STBC are transmitted from two transmit antennas over two symbol periods. The first symbol period has two symbols *x1* and *x2*, simultaneously transmitted, while during the second symbol period, these symbols are transmitted again but as *-x2** from the first antenna and *x1** from the second. We used the orthogonal space-time block code (OSTBC) encoder in the MIMO library of the MATLAB/Simulink communication system toolbox [24] to encode the input data and the OSTBC decoder to extract the symbols that were encoded. This algorithm has been experimentally demonstrated in [25, 26] to reduce error performance in the unstable wireless fading channel but not in a DAS or RoF-supported system.

MIMO schemes use spatial multiplexing to achieve higher data rates by transmitting separate data via multiple antennas at the same time to multiple receivers. The challenging task for the receiver is to detect the separate data. Simple linear detection algorithms, can restore the separated data. Such algorithms treat all transmitted signals as interference except for the desired signals from the target transmit antennas [20]. An evaluation of some detection schemes in [27] has shown that the zero-forcing linear detection algorithm which is the simplest algorithm for MIMO can produce similar error rate performance to the V-BLAST Vertical-Bell Laboratories Layered Space-Time (V-BLAST) detection algorithm that is adopted for MIMO in many recent standards. In our MIMO experiment, we wrote a MATLAB script based on the zero forcing detection weight matrix in [20] that nullifies the interfering signal and decodes separately the data sent from each transmit antenna. The weighting matrix however, relies on the decorrelated channel state information to remove the effect of inter-symbol interference.

IV. Experimental Setup

Fig. 2 shows the setup of the downlink multi-antenna scheme experiment. The baseband signal was processed offline using MATLAB/Simulink software. Pseudo-random data symbols of 88.614MSps were generated and converted to parallel sets of symbols for the 16-QAM-OFDM processing. The OFDM signal processing includes 512 IFFT size, 8 pilot subcarriers for phase tracking, 112 guard bands (zero padding) including 1 DC subcarrier, and $\frac{1}{8}$ CP size; 304 OFDM symbols were transmitted including 1 OFDM preamble symbol used for channel estimation (other parameters are given in Table 1).

The I/Q samples were downloaded onto the Tektronix Arbitrary Waveform generator (AWG) 7122C channels (channel 1 and 2) using RFXpress software running on the AWG, the sample rate was set to 195.31 MHz and the signal upconverted to RF at a carrier frequency of 2.4GHz. The amplitude of the signal from the AWG was set to 0.112Vp-p (equivalent to -15dBm) to ensure the signal is operating in the linear region of the connected Mini-Circuit amplifiers (ZX60-

TABLE I
OFDM SIGNAL PARAMETERS

Parameters	Values
Carrier Frequency	2.4GHz
IFFT Length	512
Guard bands (zero padding)	111
DC subcarrier	1
Number of Pilots	8
CP size	1/8
Bandwidth	152MHz
DL transmit power	+11dBm
UL transmit power	+3 dBm
Antenna Gain	9dBi
RoF link gain	-25dB
Symbol rate	88.614MSps

2522M+) with a further 10dB power back off due to peak-to-average power (PAPR) OFDM requirement. The amplifiers were biased to produce 20dB gain and the RF signal was directly modulated onto a distributed feedback (DFB) laser diode.

The optical signals were transmitted over 25-m length single mode fibers (SMF) from the central unit to a separate testing room, as shown in Fig. 3. The RAUs placed in the testing room consist of photodiodes biased at -5V for direct detection and connected to Mini-Circuits amplifiers (ZX60-2531M+) biased to produce 28dB gain, increasing the signal level before wireless transmission. The transmit power before the antenna is +8dBm and the antenna gain is approximately 9dBi.

The testing room layout in Fig. 3 represents a typical office, fitted with common office furniture (desks, chairs, shelves) and computers. The room is 9.7 by 8.6 m enabling large antenna separation and different receive antenna positions. The RAUs were placed on a wooden platform extension in the front of the room so that the signals were generally radiating above the desktops. The receiver, a Tektronix DPO 72304DX (Oscilloscope) was used to capture the OFDM signal at different positions in the room (positions A1 to A4 in the front row and B1 to B4 in the back row). The received OFDM signals are then amplified with low noise figure RF amplifiers.

The offline processing of the baseband complex signal captured at the DPO includes: OFDM time synchronization and demodulation, least square (LS) channel estimation using the preamble symbol, phase tracking using the pilot subcarriers (and then removing them) and signal combining/detection (depending on the multi-antenna scheme). The OFDM demodulation process involves removing the CP, guard bands (zero padding) and DC subcarrier leaving the pilot and data symbols for channel estimation and detection.

Fig. 4 shows the uplink experiment modification to the setup of Fig 2. This setup for the 1x2 SIMO scheme experiment is the

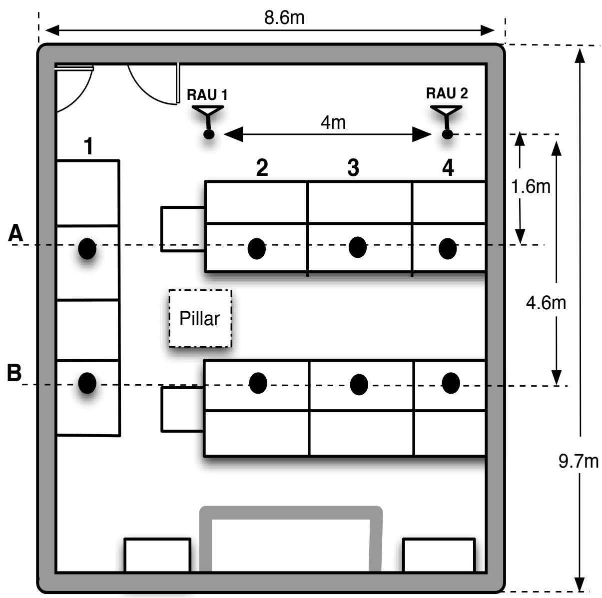

Fig 3. Testing room layout, an open plan office. A, B (1-4) represent the positions of the mobile user (the Oscilloscope/AWG)

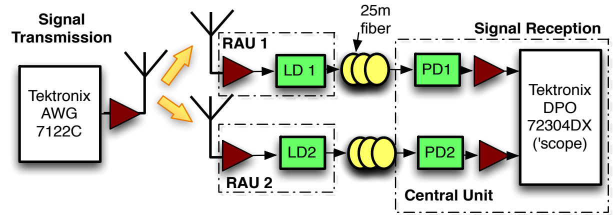

Fig. 4 The uplink experimental setup for 1x2 SIMO over Fiber

reverse of the downlink experimental setup. The transmitted signal was processed using the same steps and parameters as the downlink but the Tektronix AWG 7122C was now at the mobile unit positions and the RF signals at the RAUs brought back to the Tektronix DPO 72304DX receiver which was in the central unit. Once again, amplifier gains were set to use the linear region of the laser diode and at the point where the received signal would experience less noise and distortion. Both laser diodes were connected to 25-m lengths of single mode fiber (SMF) and then to the photodiodes in the CU. The RoF link, consisting of the direct modulated laser, optical fiber and direct detection Photodiode (PD) had a loss of 25dB, therefore a Mini-Circuits amplifier (ZX60-242GLN+) before the oscilloscope is used to boost the received signal. The received signals are saved in MATLAB format in the oscilloscope so that they can be demodulated offline and combined using the MRC algorithm.

V. Measurement Results

The results in Fig.5 show EVM measurements for the SISO system with the mobile unit placed at position A3, the closest position to the RAU. The experimental setup for downlink and uplink are different as shown in Fig. 2 and 4 which is typical for most bi-directional RoF links, [28],[29] therefore they both require separate optimization and the imperfect curve is due to the linearity of the amplifier. From Fig. 5, it can be seen that the lowest downlink EVM of 11.7% is achieved at +11dBm transmit power, and the lowest uplink EVM of 10% is achieved at +3dBm transmit power. To compare the multi- antenna schemes with SISO, the overall transmit power is kept the same.

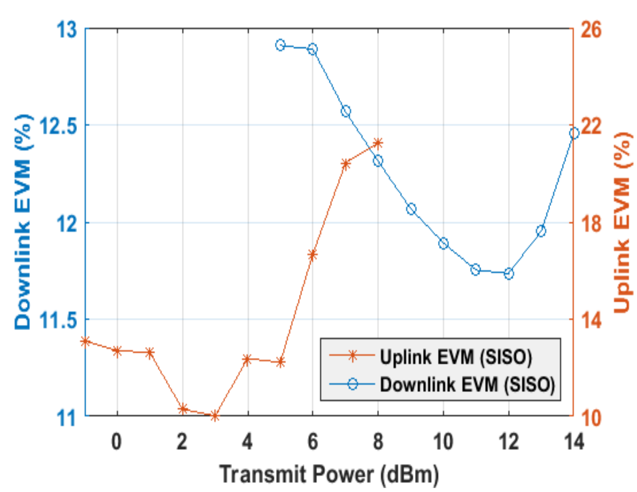

Fig 5. EVM of downlink and uplink signal transmitted from the RAU as the transmit power is increased to determine the optimum transmit power for measurement.

A. *EVM and SER*

The EVM and SER of SIMO and MISO scheme experiments are shown in Figs. 6 and 7. The measurements were taken when the inter-RAU distance was approximately 0.3m and 4m to examine the performance of the schemes with close and large antenna separation. The results were obtained as the mobile unit was moved around the testing room (shown in Fig. 3) to the different positions indicated.

From Fig. 6 it can be seen that the EVM and SER of the uplink 1x2 SIMO scheme are reduced compared to the SISO system when the RAUs were placed closely together (0.3m separation) through the MRC processing algorithm. However, the algorithm provides even better performance with the larger RAU separation of 4-m.

Similarly, in Fig. 7, it can be observed that the EVM and SER for the MISO system are reduced at all positions compared to that measured for the SISO system due to the Alamouti STBC algorithm, even when the RAUs are close (0.3m separation). When the RAUs are separated by 4m, there is a consistent and significant further reduction in EVM and SER. It should be noted that for the 0.3m separation the EVM in some positions is above the 11.2% limit for 16-QAM, while all measurements taken for the 4m separation case were within the limit.

Generally, SIMO and MISO are diversity schemes designed to improve the performance of conventional SISO wireless links. MIMO, on the other hand, may be used to increase the data rate of the system. The EVM and SER performance of the zero-forcing MIMO algorithm with RoF-DAS infrastructure and inter-RAU distances of 0.3m and 4m are shown in Fig. 8. These results show that when the RAUs are placed close together, EVM and SER are worse than for SISO in most receiver positions. When the inter-RAU distance is 4-m, the EVM is reduced in all receiver positions, below the required 11.2% limit for 16-QAM modulation. It can be seen, therefore, that obtaining any improvement with MIMO is very dependent on the channel decorrelation.

For comparison purposes, EVM results at 4m RAU spacing for all three schemes are compared in Fig. 9 noting that the overall transmit power is the same. The results show generally higher EVM for zero-forcing MIMO than the other schemes due to a trade-off between diversity gain and multiplexing gain for multi-antenna schemes, the algorithms that maximize one of the gains can hardly maximize the other simultaneously. Also, zero-forcing, only removing inter symbol interference (ISI), is ideal only in noiseless channels since it does not consider noise in data detection. However, it is often used in MIMO schemes since it is the simplest algorithm to implement and is suitable for a RoF-DAS infrastructure when signal-to-noise ratio (SNR) can be increased due to lower path loss. The main objective of the algorithm is increased data rate, which is discussed in the following.

B. *Capacity Result*

Fig. 10 shows the MER and corresponding capacity, MER is calculated after the signal combining, and the capacity is from (3), of the downlink MISO Alamouti scheme. Small improvements in capacity corresponding to the improvements in MER are evident for MISO compared to SISO and when the RAU separation is increased. As capacity has a logarithmic

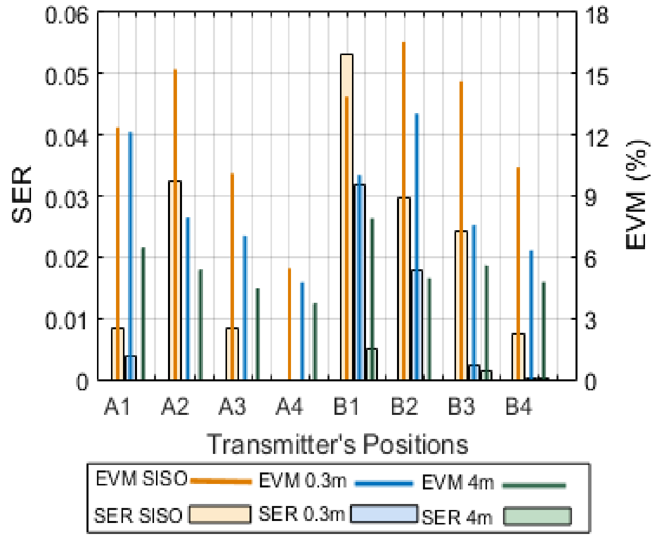

Fig. 6. SER and EVM of uplink **1x2 SIMO** measured at inter-RAU distance of 0.3m and 4m at different positions compared to **SISO**

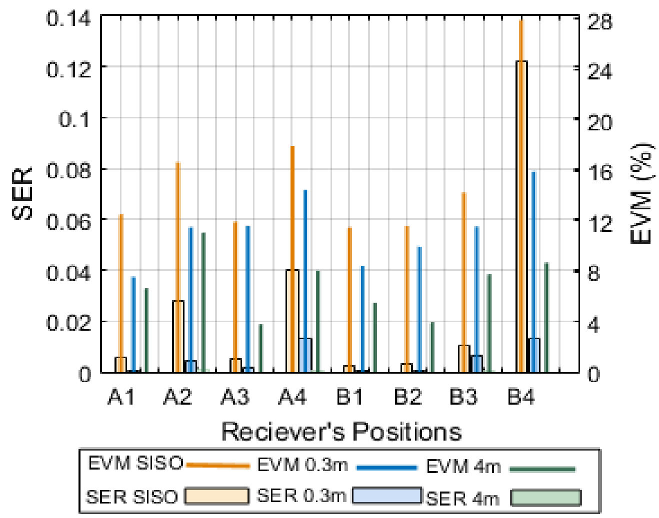

Fig. 7. SER and EVM of downlink **2x1 MISO** measured at inter-RAU distance of 0.3m and 4m at different positions compared to **SISO**

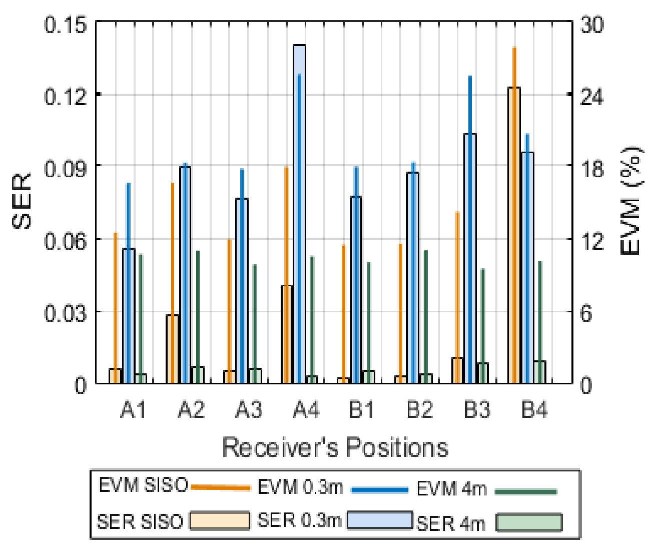

Fig. 8. SER and EVM of downlink **2x2 MIMO** measured at inter-RAU distance of 0.3m and 4m at different positions compared to **SISO**

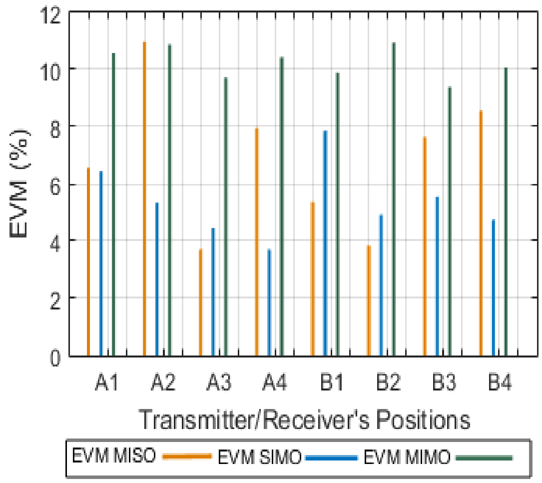

Fig. 9. EVM of **MISO. SIMO and MIMO** measured at inter-RAU distance 4m at different positions A, B (1-4)

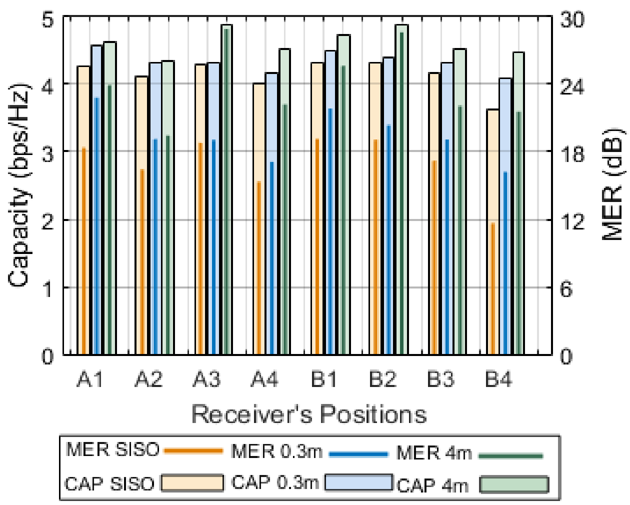

Fig. 10. Capacity and MER of downlink **2x1 MISO** measured at inter-RAU distance of 0.3m and 4m at different positions compared to **SISO**

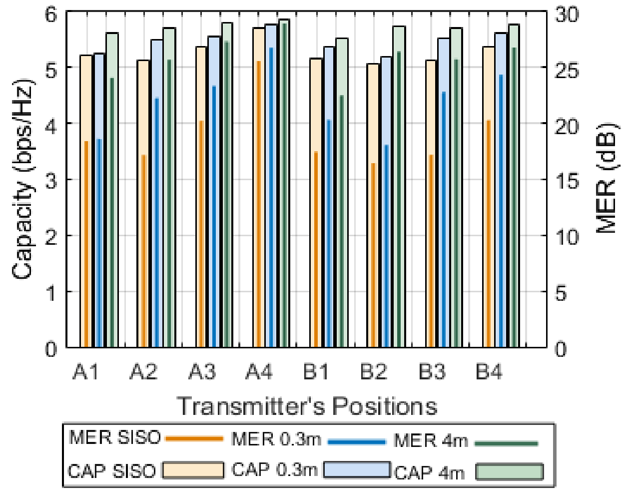

Fig. 11. Capacity and MER of downlink **1x2 SIMO** measured at inter-RAU distance of 0.3m and 4m at different positions compared to **SISO**

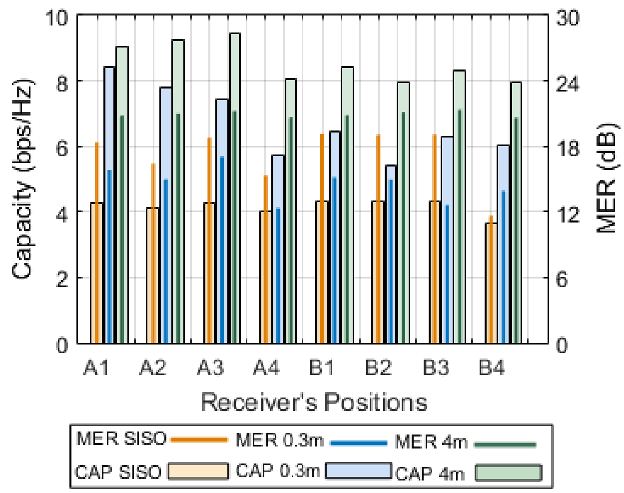

Fig. 12. Capacity and MER of downlink **2x2 MIMO** measured at inter-RAU distance of 0.3m and 4m at different positions compared to **SISO**

dependence on SNR (MER), the increases are not as significant as the linear EVM and SER reductions shown in Fig.7.

The MER and capacity, using (2), of the uplink 1x2 SIMO MRC scheme are shown in Fig. 11. Again, small but consistent improvements in capacity can be seen for the SIMO compared to the SISO system, using (3), especially with the larger RAU separation. However, this is still a logarithmic gain, and to improve the capacity linearly, we examine the 2x2 MIMO scheme that is expected to provide pure multiplexing gains.

The MER and resultant capacity, using (1), for 2x2 MIMO using the zero-forcing algorithm and compared to SISO are shown in Fig.12. The capacity of SISO results from a lower MER than in the MIMO case, as in the latter case there is often a nearer RAU to increase the performance for each link, as well as the enhancement from the multiplexing gain, which increases for greater RAU separation. It can be observed, from some of the 0.3m separation results, at least, that capacity increase can be achieved even with lower SNR (MER) than in the SISO case, because of the spatial multiplexing gain.

Fig. 13 compares the MER and capacity results for all three schemes when the inter-RAU distance is 4-m, again noting that overall transmit power is the same. The capacity for SIMO is higher than that for MISO in all positions, even in positions where the MER is inferior, due to the improvement of effective SNR by the multiple antennas. MIMO offers the highest capacity due to its spatial multiplexing.

VI. Conclusion

For the first time, the benefits of increased antenna spacing in a RoF-DAS when *comparing* specific multi-antenna transmit/receive schemes and a SISO system has been demonstrated. It has been shown that a wireless 1x2 SIMO uplink when the signals from two RAUs are RoF-transported and then centrally processed using MRC shows significantly reduced SER and a small capacity improvement due to reduced EVM/MER. A wireless MISO downlink with the signals RoF-transported and then transmitted from two RAUs using the Alamouti STBC scheme also shows significantly reduced SER and modestly increased capacity due to lower EVM/MER. For a downlink 2x2 wireless MIMO where signals are RoF-transported and transmitted from two RAUs to one mobile unit with two receiving antennas, SER can be reduced due to reduced EVM/MER (through a reduction in ISI), and spatial multiplexing gain with increased RAU spacing, leading to much increased capacity. Future work will demonstrate these

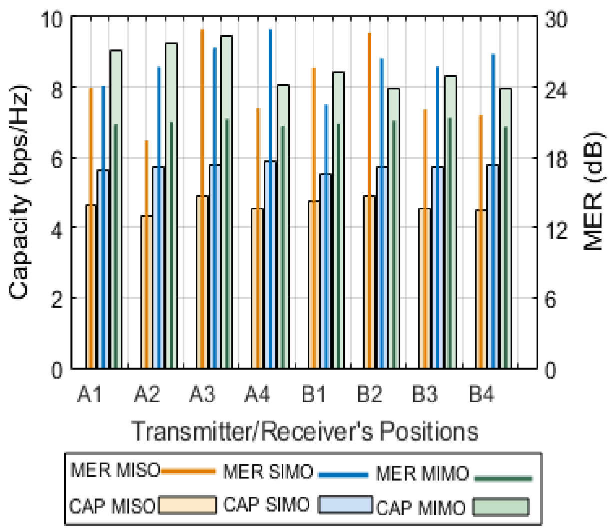

Fig. 13. Capacity and MER of **MISO, SIMO and MIMO** measured at inter-RAU distance of 4m at different positions

principles using wider bandwidths, and examine performance when millimeter-wave wireless channels are considered.

ACKNOWLEDGMENT

The authors are grateful to Dr. Anthony Nkansah and Dr. Philippos Assimakopoulos for advice on the measurements.

REFERENCE

[1] Cisco. (2015). Cisco Visual Networking Index: Global Mobile Data Traffic Forecast Update

[2] C. Fengming and F. Zhong, "Joint proportional fair user scheduling for in building distributed antenna systems," *IET Communications*, vol. 7, pp. 1802 - 1809, 2013.

[3] N. J. Gomes, P. P. Monteiro, and A. Gameiro, Next Generation Wireless Comunications Using Radio over Fiber: John Wiley & Sons, Inc., 2012.

[4] G. S. D. Gordon, M. J. Crisp, R. V. Penty, and I. H. White, "Experimental Evaluation of Layout Designs for 3 x 3 MIMO-Enabled Radio-Over-Fiber Distributed Antenna Systems," *IEEE Trans on Veh. Technol*., pp. 643 - 653, 2014.

[5] T. Alade, H. Osman, and M. Ndula, "In-Building DAS for High Data Rate Indoor Mobile Communication," presented at *the IEEE 75th Veh. Technol. Conf*., Yokohama, 2012. pp. 1-5

[6] E.M. Vitucci, L. Tarlazzi, F. Fuschini, P. Faccin, and V. Degli-Esposti, "Interleaved-MIMO DAS for Indoor Radio Coverage: Concept and Performance Assessment," *IEEE Trans. on Antennas and Propag*., vol. 62, pp. 3299 - 3309, 2014.

[7] A. Chowdhury, H. Chien, S. Fan, J. Yu, and G. Chang, "Multi-Band Transport Technologies for In-Building Host-Neutral Wireless Over Fiber Access Systems," *J. Lightwave Technol*, vol. 28, pp. 2406 - 2415, 2010.

[8] Y. Fan, A. E. Aighobahi, N. J. Gomes, K. Xu, and J. Li, "Performance analysis of commercial multiple-input-multiple-output access point in distributed antenna system," *Opt. Express*, vol. 23, pp. 500-7513 2015.

[9] A. Das, A. Nkansah, N. J. Gomes, I. J. Garcia, J. C. Batchelor, and D. Wake, "Design of Low-Cost Multimode Fiber-Fed Indoor Wireless Networks," *IEEE Trans. on Microw. Theory and Techn*, vol. 54, pp. 3426 - 3432, 2006.

[10] A. Attar, H. Li, and V. C. M. Leung, "Applications of Fiber-connected Distributed Antenna Systems in Broadband Wireless Access*," Proc. Int. Conf. on Computing, Networking and Commun*. Maui, HI. pp. 623 - 627, 2012.

[11] T. T. Higashino, T. Yamakami, K. Tsukamoto, and S. Komaki, "Link quality based MIMO antenna selection in RoF ubiquitous antenna," presented at the *IEEE Top. Meet. on Microw. Photon, Montreal*, QC, 2010. pp. 331-334

[12] K. Zhu, M. J. Crisp, H. Sailing, R. V. Penty, and I. H. White, "MIMO system capacity improvements using radio-over-fibre distributed antenna system technology," presented at the *Opt. Fiber Commun. Conf. and Exposition and the National Fiber Opt. Engineers Conf*., Los Angeles, CA, 2011.pp. 1-3

[13] F. Diehm, J. Holfeld, G. Fettweis, N. J. Gomes, D. Wake, A. Nkansah, et al., "The FUTON prototype: Broadband communication through coordinated multi-point using a novel integrated optical/wireless architecture," presented at the *IEEE Globecom Workshops*, Miami, FL, 2010.

[14] L. Cheng, M. M. U. Gul, F. Lu, M. Zhu, J. Wang, M. Xu, et al., "Coordinated Multipoint Transmissions in Millimeter-Wave Radio-Over-Fiber Systems," *J. Lightwave Technol*, vol. 34, pp. 653 - 660, 2016.

[15] A. E. Aighobahi, P. Assimakopoulos, and N. J. Gomes, "Experimental analysis of single and multiple antenna units in uplink of radio-over-fiber distributed antenna system," in *IEEE Int. Top. Meet. on Microw. Photon*. ed. Paphos, Cyprus, 2015, pp. 1-4.

[16] C. D. Ziomek and M. T. Hunter. (2012). Extending the Useable Range of Error Vector Magnitude (EVM) Testing

[17] D. Tse and P. Viswanath, Fundamentals of wireless communication: Cambridge University Press, 2005.

[18] R. Hranac, BER and MER Fundamentals: Cisco Systems, 2007.

[19] C.Langton and B.Sklar. (2011). Finding MIMO - Complex To Real. Available: complextoreal.com

[20] Y. Cho, J. Kim, W. Yang, and C. G. Kang, MIMO-OFDM Wireless Communications with MATLAB: John Wiley and Sons Ltd, 2010.

[21] G. E. Corazza, V. Degli-Esposti, M. Frullone, C. Passerini, and G. Riva, "Performance evaluation of space diversity in indoor communications using a ray-tracing propagation model " presented at the *Int. Symposium on Personal, Indoor and Mobile Radio Commun*., Toronto, Ont., 1995.

[22] S. Sharma and R. Khanna, "Spatial Diversity with LDPC Codes," presented at the *IEEE GLOBECOM Workshops*, New Orleans, LO, 2008.

[23] S. Alamouti, "A simple transmit diversity technique for wireless communications," *IEEE J. on Sel. Areas in Commun*., pp. 1451 - 1458.

[24] MATLAB version R2015a. Communication Toolbox: The MathWorks Inc., 2015

[25] J. A. Garcia-Naya, T. M. Fernandez-Carames, H. J. Perez-Iglesias, M. Gonzalez-Lopez, L. Castedo, D. Ramirez, et al., "Performance of STBC transmissions with real data " presented at the *Mobile and Wireless Commun. Summit,* Budapest, 2007.

[26] F. J. Vazquez-Araujo, J. A. Garcia-Naya, M. Gonzalez-Lopez, L. Castedo, and J. Garcia-Frias, "Experimental evaluation of MIMO coded modulation systems: Concatenation with OSTBC or spatial multiplexing " in *Int. Conf. on Sys., Signals and Image Processing*, Vienna, 2012, pp. 93-96.

[27] O. C. Oghre and S. Salous, "BER performance evaluation of HF MIMO spatial multiplexing systems," presented at the *URSI General Assembly and Scientific Symposium*, Beijing, 2014.

[28] J. A. Altabas, J. A. L. D. Izquierdo, A.Lerin, F. Sotelo, and I. Garces, "1Gbps full-duplex links for ultra-dense-WDM 6.25GHz frequency slots in optical metro-access networks," *Opt. Express,* vol. 24, pp. 555-565, 2016.

[29] Z. Al-Qazwini and H. Kim, "Symmetric 10-Gb/s WDM-PON Using Directly Modulated Lasers for Downlink and RSOAs for Uplink," *J. Lightwave Techno*l, vol. 30, pp. 1891 - 1899, 2012.

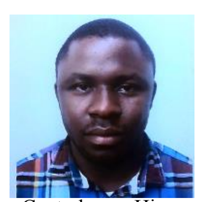

Anthony E. Aighobahi received a B.Sc. (Hons.) degree in Computer Science and Information Technology from Igbinedion University, Nigeria in 2009 and a Masters degree in Electronic Engineering from Manchester Metropolitan University in 2012 and is currently working towards the PhD degree in Electronic Engineering at the University of Kent, Canterbury. His research involves the experimental investigation of MIMO schemes for RoF-DAS.

Nathan J. Gomes (M'92–SM'06) received the B.Sc. degree from the University of Sussex, Sussex, U.K., in 1984, and the Ph.D. degree from University College London, London, U.K., in 1988, both in electronic engineering.

From 1988 to 1989, he held a Royal Society European Exchange Fellowship with ENST, Paris, France. Since late 1989, he has been with the University of Kent, Canterbury, U.K., where he is currently Professor of Optical Fibre Communications. His current research interests include fiber-wireless access, and RoF systems and networks.

Professor Gomes was a TPC Co-chair for the MWP 2014 IEEE Topical Meeting in Sapporo and TPC Chair for IEEE International Conference on Communications, ICC 2015 in London.